Enhanced Power System Stability
by Coordinated PSS Design

Adam Dyśko, *Member, IEEE*, William E. Leithead, and John O'Reilly, *Senior Member, IEEE*

Abstract—A step-by-step coordinated design procedure for power system stabilisers (PSSs) and automatic voltage regulators (AVRs) in a strongly coupled system is described in this paper. It is shown that it is possible to separate the design of individual PSSs and separate the design of individual AVRs. Thereby, the designs of AVR and PSS devices at a given machine can be coordinated to achieve near-optimal overall power system stability performance, including oscillation stability performance and transient stability performance. The proposed coordinated PSS/AVR design procedure is established within a frequency-domain framework and serves as a most useful small-signal complement to established large-signal transient simulation studies.

Index Terms—Multimachine systems, oscillation mode stabilization, power system stabiliser (PSS) and automatic voltage regulator (AVR) design, transient stability.

I. INTRODUCTION

TWO of the most important design criteria for multimachine power systems are transient stability and damping of electromechanical modes of sustained oscillation [1]–[3]. These two design criteria have assumed even greater importance in the wake of recent interconnection blackouts in the U.S., Canada, and Europe [4]. The focus has almost exclusively been on the second criterion, oscillation instability as cured by suitably tuned power system stabilisers (PSS) attached to appropriate generators [5]–[22]. Particular emphasis is given to the performance of PSS devices [5], [6], but without direct reference to the performance of interacting generator automatic voltage regulator (AVR) devices.

On the contrary, this paper deals with overall power system stability, i.e., both the system transient stability as provided by the AVR devices and the system oscillation stability/damping as provided by the PSS devices. A significant extension of previous work [7] to multimachine systems, the necessary coordination of separate AVR and PSS devices to achieve the limits of overall system stability performance, is developed in this paper through the extensive use of small-signal Bode frequency-response design methods.

The previous paper [7] dealt with the harmful interaction between AVR and PSS devices at a given machine. As is well known [1], [7], a fast-response AVR improves large-signal transient stability in the sense that it increases the ability of the power system to maintain synchronism when subjected to severe transient disturbances, for instance, network faults. Also highlighted [7] is the fact that while the detrimental effect of a fast-acting AVR at a given machine on oscillation stability is well known, the converse detrimental effect of the PSS at the same machine on transient stability is not. A recent discussion of the definitions of large-signal transient stability and small-signal oscillation stability is observed in [23]. It is established [7] that the AVR and PSS devices, suitably designed, at a given machine have roles that are separated by frequency. Namely, the AVR provides for transient stability performance by being active in the lower frequency range, while the PSS provides for oscillation stability only by being active in the higher frequency range. Lower frequency range is the frequency range up to, but short of oscillation mode frequencies, while higher frequency range is the frequency range around oscillation mode frequencies and above. At any given machine, proper AVR and PSS designs in appropriate frequency ranges to achieve the limits of transient stability and oscillation stability require minimum adverse interaction between AVR and PSS devices. This also accords with industrial experience of PSS tuning, where a limit on the lower frequency gain of the stabilizer is necessary during changes in power set point at the price of reduced stabilizer performance [8].

The salient feature of multimachine systems, however, is that loop interaction, as exemplified by the two PSS loops of the well-known five-machine equivalent of the unstable South/South Eastern Brazilian network, also needs to be taken into account, as noted by [6]. The primary objective of PSS design is oscillation-mode stabilization. Consequently, as demonstrated in this paper, even with significant interaction between PSS loops, the design of one PSS need not impact on the design of another PSS: the PSSs can be designed separately. Furthermore, as this paper also shows, there is no significant interaction between AVR loops in the lower frequency range. Consequently, both transient stability performance and stabilization of system low-frequency unstable modes can be achieved by again designing the AVRs separately. Therefore, not only is it possible to coordinate the design of the AVR and PSS devices at a given machine to achieve their separate control functions, it is also possible to separately coordinate the designs of the AVRs and coordinate the designs of the PSSs to achieve the limits of overall stability performance in strongly
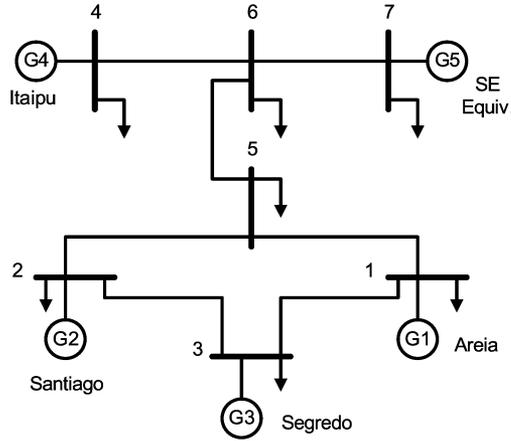
Fig. 1.   South/Southeast Brazilian equivalent test system.

TABLE I
FIVE NETWORK IMPEDANCE SCENARIOS

Case #	1	2	3	4	5
$X_{5\text{-}6}$ pu	0.39	0.50	0.80	0.39	0.39
$X_{6\text{-}7}$ pu	0.57	0.57	0.57	0.63	0.7
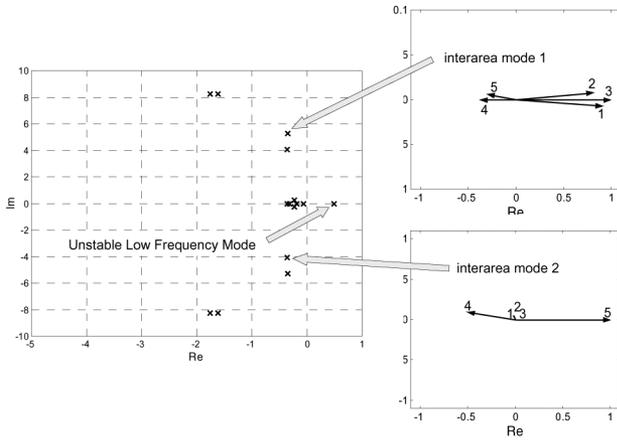
Fig. 2.   Uncontrolled system modes of oscillation (without AVRs or PSSs).

Fig. 3.   Closed-loop system modes of oscillation with AVRs as in (1).

Fig. 4.   AVR/PSS configuration.
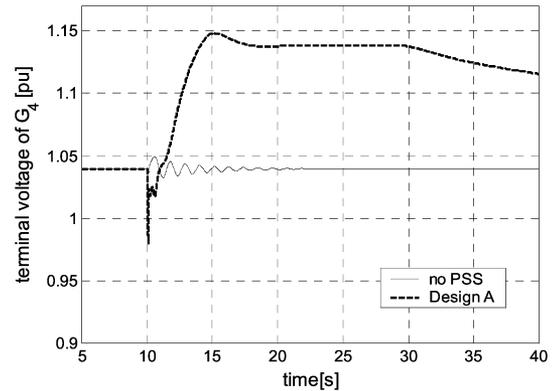
Fig. 5.   Terminal voltage response of G_4 with and without the design A PSSs.

coupled multimachine systems. This is the main contribution of this paper.

The paper is organized as follows. Section II takes as our test system the dynamically challenging unstable five-machine equivalent of the Brazilian South/South Eastern network [6], [9]. The transient stability performance need for coordinated PSS/AVR design is established in Section III by a frequency-response analysis of a two PSS designs for the test system. A coordinated PSS/AVR design with only one PSS established in Section IV, although resulting in a stable system, demonstrates the oscillation damping need for a second PSS. A step-by-step coordinated PSS design procedure is presented and applied to the two PSS designs in Section V. It is combined with a step-by-step coordinated AVR design procedure in Section VI to reconcile the design objectives of system oscillation stabilization and transient stability performance, and thereby achieve the limits of overall power system stability performance. Conclusions are presented in Section VII.
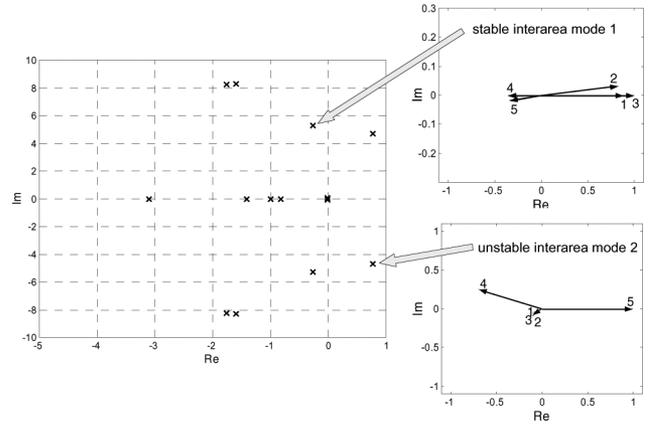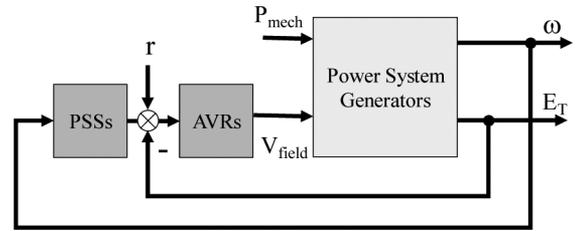
II.   TEST SYSTEM

The test system is a modified seven-bus, five-machine equivalent model of the South/Southeast Brazilian network [6], [9], as depicted in Fig. 1. The authors in [6] considered five scenarios with varying impedances $X_{5\text{-}6}$ and $X_{6\text{-}7}$ presented in Table I. In this paper, PSS/AVR design focuses on the most challenging scenario 5. However, in order to verify robustness, time-domain simulation results for all five scenarios are also considered in Section VI. Complete system data for this network can be obtained from [9].

Consider first the uncontrolled system before application of either AVRs or PSSs. The eigenvalue/eigenvector analysis of the linear system model, shown in Fig. 2, indicates that the uncontrolled system has instability caused by a very low frequency real mode. There are also two lightly damped (though stable) interarea modes: interarea mode 1 involves oscillation of the generator group G_1, G_2, and G_3 swinging against generator
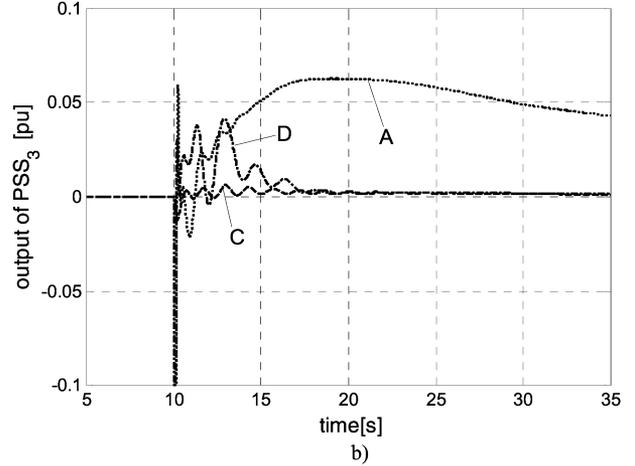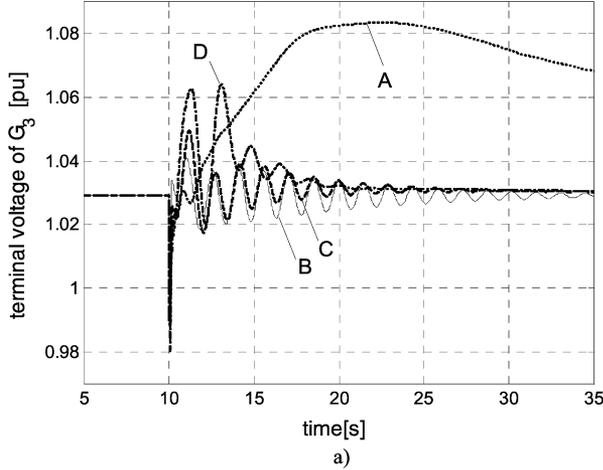
Fig. 6. Response of generator G_3 to 100 ms fault in the vicinity of node 5. (a) Terminal voltage response of generator G_3 for all four AVR/PSS designs. (b) PSS output of generator G_3 for AVR/PSS designs A, C, and D.

group G_4, G_5; interarea mode 2 involves generator G_4 swinging against generator G_5.

All generators are now equipped with an AVR having first-order transfer function [9] given by

$$\mathrm{AVR}_1(s) = \frac{30}{(1 + 0.05s)}. \tag{1}$$

AVR gains are progressively increased in designs B, C, and D, in later sections, to achieve enhanced performance.

When all AVR loops are closed, the unstable real pole is stabilized, but the interarea mode 2, involving generator G_4 swinging against generator G_5, becomes unstable, as shown in Fig. 3. This is the well-known destabilizing effect of a fast-acting AVR [1], [2]. Clearly, stabilization of the unstable interarea mode 2 at 5 rad/s, displayed in Fig. 3, is mandatory.

III. UNCOORDINATED TWO PSS/AVR DESIGNS

To prevent oscillation instability, it is a standard practice to combine the application of PSSs with fast-acting AVRs, as depicted schematically in Fig. 4.

In [6], PSSs are added to the test system at generator G_3 (Segredo) and generator G_4 (Itaipu). Four different designs for the PSSs are discussed, but given that none performs markedly better than the others, we only consider one of the designs here: the classical design [6], designated design A in this paper, consisting of two conventional double-lead PSSs with the following transfer functions (2) and (3).

Segredo G_3 PSS design A:

$$\mathrm{PSS}_3(s) = 30 \times \frac{3s}{1 + 3s} \times \frac{(1 + 0.3s)}{(1 + 0.02s)} \frac{(1 + 0.1s)}{(1 + 0.008s)}. \tag{2}$$

Itaipu G_4 PSS design A:

$$\mathrm{PSS}_4(s) = 60 \times \frac{3s}{1 + 3s} \times \frac{(1 + 0.3s)}{(1 + 0.03s)} \frac{(1 + 0.3s)}{(1 + 0.03s)}. \tag{3}$$

All PSSs in this paper including (2) and (3) feedback generator speed ω as an auxiliary signal to the exciter/AVR voltage input of the generator to which the PSS is attached, as depicted in

Fig. 4. There is no coordination of the PSS designs (2) and (3) in design A with the AVRs (1).

The dynamic performance of design A and other PSS designs, progressively introduced in Sections IV–VI of this paper, are verified by nonlinear simulation in the PSS/E software package. More detailed models of AVR and PSS, ST3A excitation system and PSS1A, respectively [22], are used in all simulations; see Appendix A for parameter values used. A symmetrical three phase fault of 100-ms duration is simulated in the vicinity of node 5, followed by the clearance and disconnection of the 250 MW load. This large-signal network disturbance event is equivalent to a system fault on an adjacent outgoing feeder, leading to the loss of part of the load connected to that node.

Although, as already mentioned, it is well known that improving transient stability, through the use of fast-acting AVRs, may reduce oscillation stability, it is less well known that improving oscillation stability, through the use of PSSs, may, in turn, reduce the effectiveness of the AVRs, [7]. To illustrate this effect, the scenario is initially modified to be stable without the two PPSs being present by reducing all the loads by 20% of their original value. The G_4 terminal voltage response of the system with and without the PSSs is shown in Fig. 5. Although the PSSs successfully damp the interarea mode, they have impaired the AVRs to recover the terminal voltage: the recovery is very slow.

The recovery responses in terms of voltage and PSS output for the fully loaded system are shown in Figs. 6 and 7 for generator G_3 and G_4, respectively.

In [6], damping of the interarea mode, i.e., oscillation stability, is the objective for the PSS design. It can be seen from Figs. 6 and 7 that, by this criterion, the performance of design A is good. However, the reduction in the effectiveness of the AVRs is again evident from the slow recovery of the terminal voltages following the 100-ms fault.

The most direct way of confirming that the source of the poor system transient response for design A is indeed the PSSs is through the small-signal frequency response of the open-loop generator G_4 PSS channel [7], PSS channel 2 shown in Fig. 8(a). With PSS_4 attached to generator G_4, open-loop generator PSS
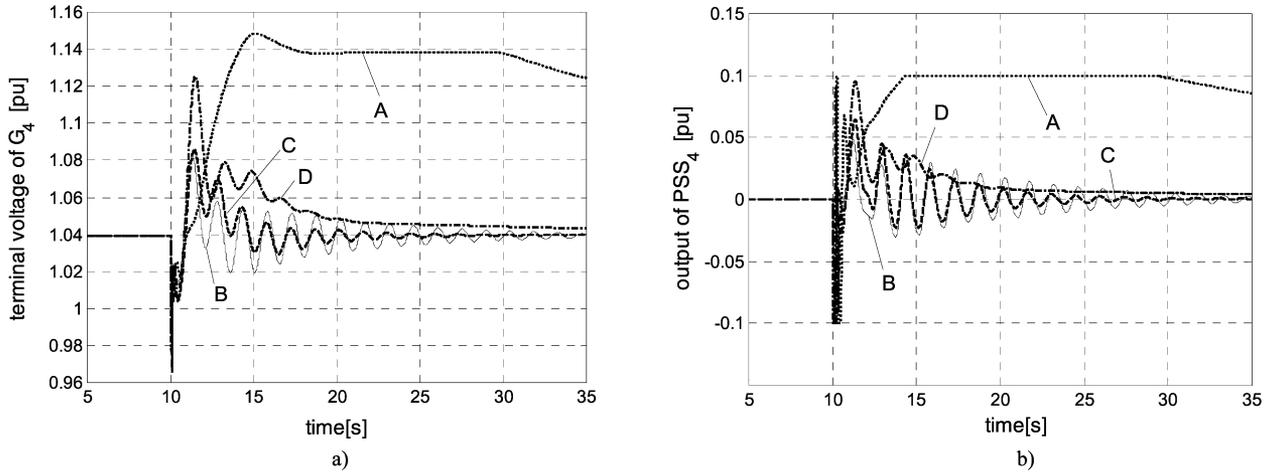
Fig. 7. Response of generator G_4 to 100 ms fault in the vicinity of node 5. (a) Terminal voltage response of generator G_4 for all four AVR/PSS designs. (b) PSS output of generator G_4 for all four AVR/PSS designs.
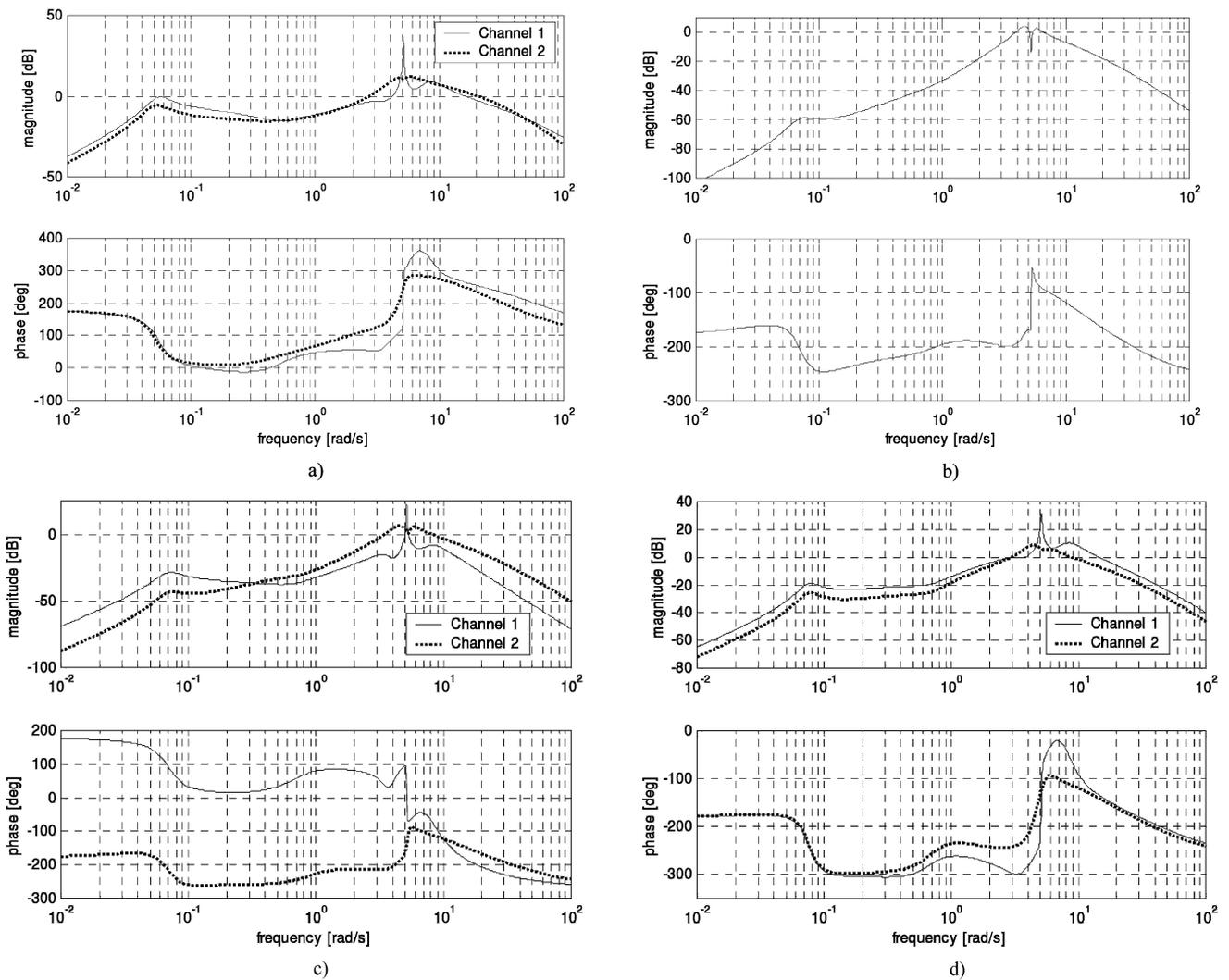
Fig. 8. Bode plots for AVR/PSS designs A–D. (a) Design A. (b) Design B. (c) Design C. (d) Design D.

channel 2 is defined [7] as the response between AVR_4 input and generator G_4 output speed with the PSS_4 loop open, PSS_3 loop closed, and all four AVR loops closed. Open-loop gener-

ator PSS channel 1 for PSS_3 attached to generator G_3 is similarly defined. The corresponding stability margins are listed in Table II.

TABLE II
STABILITY MARGINS FOR AVR/PSS DESIGNS A–D

Solution	Gain stability margins		Phase stability margins	
	Amplitude [dB]	Frequency [rad/s]	Angle [deg]	Frequency [rad/s]
A	Ch. 1 36.0	Chan. 1 5.11	Chan. 1 92.7	Chan. 1 4.16
	Chan. 2 10.8	Chan. 2 4.44	Chan. 2 62.4	Chan. 2 2.73
B	3.68	4.49	14.9	3.94
			11.7	5.05
			122.0	5.41
			86.7	6.62
C	Chan. 1 20.5	Chan. 1 14.7	Chan. 1 83.4	Chan. 1 4.97
			112	5.32
	Chan. 2 6.82	Chan. 2 4.68	Chan. 2 33.3	Chan. 2 3.47
			69.7	8.18
D	Chan. 1 30.8	Chan. 1 5.05	Chan. 1 111	Chan. 1 3.75
			45.8	14.6
	Chan. 2 8.76	Chan. 2 4.46	Chan. 2 62.7	Chan. 2 2.96
			66.7	8.96

Fig. 9. Bode plots of transfer functions between voltage reference and speed.

To increase the damping and stabilize the interarea mode at 5 rad/s, the gain of the open-loop PSS channel 2 Bode plot must be raised above 0 dB at 5 rad/s by the PSS [7]. From Fig. 8(a), it is clear that this is achieved by design A, but the gain of the channels also remains near 0 dB over an extended range of lower frequencies 0.05–5 rad/s, thereby seriously degrading the transient stability performance of the AVRs over that frequency range [7]. To preserve the effectiveness of the AVRs, the gains of the open-loop PSS channels should be much less than 0 dB away from the interarea mode frequency [7], i.e., the parameters of the PSS should be chosen such that this is the case.

The earlier fundamental limiting tradeoff between AVR design in the lower frequency range (up to, but short of interarea mode frequency 5 rad/s) to achieve transient stability and PSS design in the higher frequency range (around the interarea mode frequency 5 rad/s and above) to achieve system oscillation mode stability and damping is highlighted in [7]. If the limits of overall power system stability performance are to be achieved, coordination of the designs of the PSSs with the AVRs is required and progressively explored in three new coordinated designs in Sections IV–VI.

IV. COORDINATED SINGLE PSS/AVR DESIGN

The focus in design B is on the same pair of generators as in Section III, namely, G_3 and G_4, but with only one PSS, applied to the system at generator G_4. The Bode plots of the transfer functions, between the voltage reference input r and speed ω (refer to Fig. 4), with no PSSs present are shown in Fig. 9 for each generator. Only for generator G_4 is the interarea mode at 5 rad/s not accompanied by right half-plane zeros. (The signature is the sharp increase in phase at 5 rad/s [7].) Hence, a single PSS at generator G_4, but at no other generator, can stabilize the system. Unlike Section III, the PSS design is coordinated with the AVR at generator G_4 in design B to achieve oscillation stability without reducing transient stability.
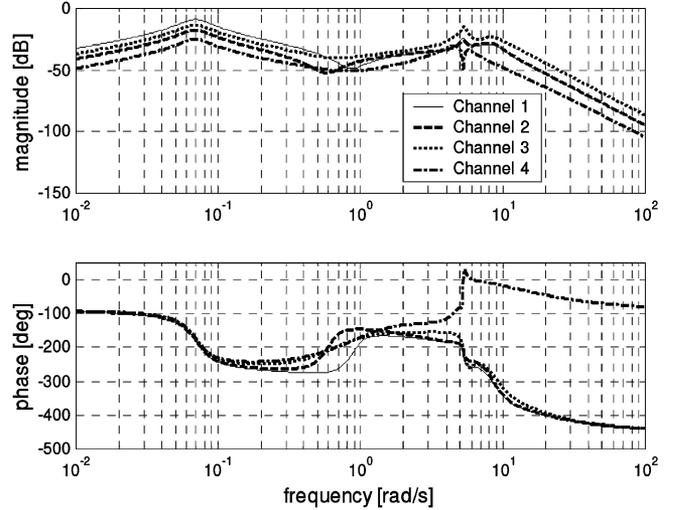
Keeping the design of AVR_4 unchanged with transfer function (1), the parameters for PSS_4 are chosen to keep the gain of the open-loop generator PSS_4 channel above 0 dB at 5 rad/s, but the gain much less than 0 dB at lower and higher frequencies, see Fig. 8(b). The design of PSS_4 is thus coordinated with AVR_4, thereby, as discussed in Section III, ensuring oscillation stability while minimizing any degradation in the transient stability performance of AVR_4. The resulting design of the PSS at generator G_4 has the transfer function

$$\text{PSS}_4(s) = 0.15 \times \frac{1.25s}{1 + 1.25s} \times \frac{(1 + 10s)}{(1 + 1.25s)} \frac{(1 + 10s)}{(1 + 0.033s)} \quad (4)$$

where the washout constant of a PSS is smaller than the usual range 3–10 s, as in (4); this is so that it does not interfere with phase compensation in the electromechanical mode range.

In design A, AVR_4, the AVR for generator G_4, is faster acting than AVR_3, the AVR for generator G_3. Since the designs for the PSSs on both generator G_3 and G_4 are being investigated here, each needs to be treated equitably. Hence, to compensate for AVR_4 being faster acting than AVR_3, the parameters for AVR_3 are adjusted so that its transfer function becomes

$$\text{AVR}_3(s) = \frac{2.8 \times 30}{(1 + 0.05s)}. \quad (5)$$

The overall system stability is also improved by this adjustment to AVR_3 through greater stabilization of the unstable low-frequency real mode. The transfer functions of the other AVRs remain unchanged as in (1). This equalization of the AVRs is confirmed in Fig. 10, showing the Bode plots for the open-loop generator G_3 AVR channel [7], AVR channel 1, and open-loop generator G_4 AVR channel, AVR channel 2. Open-loop AVR channel 1 is defined [7] as the response between AVR_3 input and generator G_3 output terminal voltage with AVR_3 loop open and all other AVR loops closed. Open-loop AVR channel 2 for AVR_4 is similarly defined. Through the earlier equalization, the crossover frequencies for AVR channels 1 and 2 are both roughly 5 rad/s.

Coordinated AVR/PSS design B is specified by (4) and (5). By coordinated design, we mean that the design of one device,
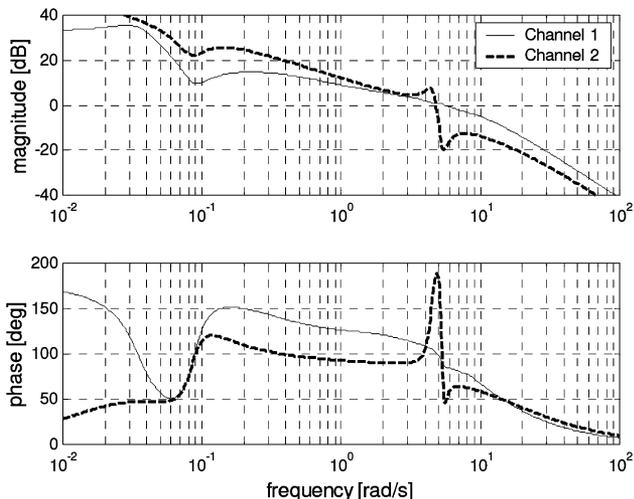
Fig. 10. AVR channels for design B.

here PSS_4, takes into account the consequences for other device or devices, here AVR_4. Its large-signal voltage and speed responses to a 100-ms fault are shown in Fig. 7. The transient stability performance of the AVR channel at generator G_4 is observed to be good. However, this coordinated AVR/single PSS design leaves the oscillatory interarea mode at 5 rad/s, rather lightly damped, giving rise to the fast ripple on the responses shown in Fig. 7. This is a consequence of the small gain by which the Bode plot of the open-loop PSS_4 channel exceeds 0 dB in the region of the interarea mode at 5 rad/s, as shown in Fig. 8(b) and the small stability margins in Table II. The latter are required to be positive for system stability. (For further discussion of the design of PSSs, see [7].) By comparing design A and design B, the performance tradeoff between the transient stability and oscillation stability is clear. Design B achieves better transient stability, but at the expense of reduced oscillation stability.

For greater overall power system stability performance than that achieved by design B, PSSs are required at both G_3 and G_4. The coordinated PSS/AVR design for PSS_3 and PSS_4 is explored in Sections V and VI.

V. COORDINATED TWO PSS DESIGN

In Section IV, to prevent degrading transient stability performance, the coordinated design with a single PSS, at generator G_4, is explored. The tradeoff between improved AVR performance and reduced oscillation stabilization by the PSS is observed. In this section, the coordinated design of the PSSs, with more than one PSS present, is discussed. With more than one PSS present, the dynamics of any particular generator can be modified by the presence of PSSs at other generators. When this modification to the dynamics is sufficient to prevent the design of a PSS in isolation, then the system is referred to as strongly coupled. The design of any PSS then depends on the design of the other PSSs. Here, in design C, PSSs are included at both generators G_3 and G_4. There is a strong coupling at 5 rad/s, and the frequency of the interarea mode and the design of PSS_3 apparently depend on the design of PSS_4 and *vice versa*. The design

of the AVR's remain unchanged from Section IV, specifically (1) and (5).

The primary objective for the PSSs is to stabilize the system. With PSS_3 and PSS_4 present, the system is two-input two-output. The following step-by-step design procedure is appropriate for a strongly coupled multimachine system, such as that of Fig. 1. It is derived from the results of [24], where the stability and performance aspects of the design of a diagonal controller for a strongly cross-coupled system are separated. Here, we focus only on the stabilization aspect.

Step-by-step design procedure for PSS_3 *and* PSS_4:

1) Check that the two-input two-output PSS system has no right half-plane transmission zeros.
2) Define the open-loop generator G_3 PSS channel, PSS channel 1, with the PSS_4 gain chosen to be infinite. (A very high gain would suffice.) This PSS channel has right half-plane zeros only when the two-input two-output PSS system has right half-plane transmission zeros. The absence of right half-plane transmission zeros in the two-input two-output PSS system can thus be confirmed.
3) Design PSS_3 so that the gain of the Bode plot for PSS channel 1 defined in 2 is raised above 0 dB at the interarea mode frequency, 5 rad/s, with sizeable stability margins while inducing rapid gain roll off at lower and higher frequencies.
4) Define the open-loop generator G_4 PSS channel, PSS channel 2, with the PSS_3 designed in step 3).
5) Design PSS_4 in a similar fashion to step 3).

The general step-by-step procedure for n-input n-output PSS systems comprising stabilizers $\mathrm{PSS}_1, \ldots, \mathrm{PSS}_n$ is presented in Appendix B.

With the PSSs designed by the earlier procedure, the closed-loop system is robustly stable [24]. The performance and stability robustness achieved by the PSS designs can be assessed from the standard PSS channels 1 and 2, defined as in Section III. In particular, PSS channel 1 is defined using the design for PSS_4 obtained in step 5). Since the cross-coupling of the two PSS channels is weak at frequencies away from the interarea mode frequency, rapid gain roll off (at lower and higher frequencies than the interarea mode) of the standard PSS channels is ensured by designing PSS_3 and PSS_4 to cause rapid gain roll off of the PSS channels defined in step 2) and step 4).

The earlier procedure forms the basis of new PSS designs at generators G_3 and G_4, with the AVR designs the same as in design B. The designs of the two PSSs are coordinated with each other. Furthermore, the design of PSS_3 is coordinated with the design of AVR_3, and the design of PSS_4 is coordinated with the design of AVR_4. The new coordinated two PSS design is designated design C.

Segredo G_3 PSS design C:

$$\mathrm{PSS}_3(s) = 0.8 \times \frac{3s}{1+3s} \times \frac{(1+3s)}{(1+0.4s)}. \qquad (6)$$

Itaipu G_4 PSS design C:

$$\mathrm{PSS}_4(s) = 0.45 \times \frac{3s}{1+3s} \times \frac{(1+10s)}{(1+2.5s)} \frac{(1+10s)}{(1+0.033s)}. \quad (7)$$

We note the similarity of the PSS_4 design (7) to that of the previous single PSS_4 design (4) in design B of Section IV. Similarly to the single PSS_4 design B in Section IV, each of the PSS_3 and PSS_4 designs raises the respective gains of the open-loop generator PSS channels 1 and 2 in the Bode plots shown in Fig. 8(c) above 0 dB *only* in the vicinity of the unstable mode frequency 5 rad/s. At all other frequencies, the gains of the open-loop generator PSS channels 1 and 2 are rolled off so as not to degrade AVR transient stability performance. In comparison to the PSS_4 design (4) in design B, PSS_4 design (7) has higher gain and is above 0 dB over a greater frequency interval for better oscillation mode damping. In Table II, damping and stabilization performance of design C is confirmed by the quite satisfactory PSS channel gain and phase margins. The improvement in overall stability performance over design B is corroborated by the large-signal voltage and speed responses to a 100-ms fault shown in Figs. 6 and 7.

The separation of the individual PSS designs through the step-by-step PSS design procedure permits each PSS design to be coordinated with the local AVR and near optimal for the existing AVRs of Section IV. Design C is close to the limit of transient stability performance. There is, however, room for oscillation damping improvement. The oscillation stability cannot be improved further by increasing the gains of the PSSs without degrading the transient stability performance. Instead, the frequency ranges over which the AVRs are active, i.e., above 0 dB, can be reduced without compromising the transient stability. The extent to which the AVRs reduce oscillation stability prior to the addition of the PSSs is thus lessened, thereby allowing improved overall stability performance of the coordinated AVR/PSS design. This approach is adopted in design D in Section VI.

VI. Coordinated Two PSS/AVR Design

In Section V, the coordinated design of the PSSs with the existing AVRs of Section IV is discussed. It is observed that the only option to further increase oscillation stability is to reduce the frequency ranges over which the AVRs are active. Of course, the transient stability performance must not be compromised by a reduction in the AVR gain in the lower frequency range below 5 rad/s. There is strong coupling at very low frequencies, below 0.1 rad/s. However, at higher frequencies, the cross-coupling is much weaker. Consequently, the AVR loops for a multimachine system, such as that of Fig. 1, can be designed *independently* of each other.

In contrast to the PSSs, the primary objective for the AVRs is the performance, i.e., for good transient stability performance, fast-acting AVRs are required. The AVRs must stabilize any low-frequency instability such as the unstable real mode in the test system, but they are not required to achieve overall system stability. Indeed, as for the test system, they may induce oscillation instability that must subsequently be remedied by the PSSs. For AVR_3 and AVR_4, the system is two-input two-output. The following step-by-step design procedure is appropriate for a strongly coupled multimachine system, such as that of Fig. 1. Again, it is derived from the results of [24], but now the focus is on the performance aspect.

Step-by-step design procedure for AVR_3 *and* AVR_4:

1) Define the open-loop generator G_3 AVR channel, AVR channel 1, with the AVR_4 gain chosen to be infinite. (A very high gain would suffice.)
2) Design AVR_3 so that the gain of the Bode plot for the AVR channel 1, defined in 2, is high and stabilizes any instability at low frequency. The frequency range over which the open-loop gain is above 0 dB must meet the requirements of the context. Here, the crossover frequency must be reduced below 5 rad/s, the frequency of the interarea mode.
3) Define the open-loop generator G_4 AVR channel, AVR channel 2, similarly to step 1).
4) Design AVR_4 in a similar fashion to step 2).

The general step-by-step procedure for *n*-input *n*-output AVR systems comprising regulators $\mathrm{AVR}_1, \ldots, \mathrm{AVR}_n$ is presented in Appendix B.

With the AVRs designed by the earlier procedure, the limit to the transient stability performance is realized. The performance achieved by the PSS designs can be assessed from the standard AVR channels 1 and 2, defined as in Section III. In particular, AVR channels 1 and 2 are defined using the designs for AVR_4 and AVR_3 obtained in step 4) and 2), respectively.

The earlier procedure forms the basis of new AVR designs at generators G_3 and G_4. Subsequently, using the step-by-step procedure of Section V, new PSS designs coordinated with the new AVR designs are obtained for the PSSs at generators G_3 and G_4. The new PSS/AVR design is designated design D.

Segredo G_3 AVR/PSS design D:

$$\mathrm{AVR}_3(s) = 4 \times \frac{30}{1+0.05s} \times \frac{(1+2.5s)}{(1+10s)} \quad (8)$$

$$\mathrm{PSS}_3(s) = 4.5 \times \frac{s}{1+s} \times \frac{(1+0.3s)}{(1+0.02s)} \frac{(1+10s)}{(1+s)}. \quad (9)$$

Itaipu G_4 AVR/PSS design D:

$$\mathrm{AVR}_4(s) = 2 \times \frac{30}{1+0.05s} \times \frac{(1+2.5s)}{(1+10s)} \quad (10)$$

$$\mathrm{PSS}_4(s) = 3.63 \times \frac{3s}{1+3s} \times \frac{(1+10s)}{(1+0.1s)} \frac{(1+0.14s)}{(1+0.03s)}. \quad (11)$$

It is observed in (8) and (10) that, compared to the previous AVR designs used in design C, the gains of AVR_3 and AVR_4 are increased at low frequency, but reduced at higher frequencies by the additional lag-lead network. By means of the PSS/AVR tradeoff, this allows improved PSS design with higher gain in the vicinity of 5 rad/s, the frequency of the interarea mode. The Bode plot of the open-loop standard AVR channels are shown in Fig. 11 together with AVR channels used in the earlier step-by-step AVR design procedure, i.e., AVR channel 1 is defined with the gain of AVR_4 infinite and AVR channel 2 is defined with
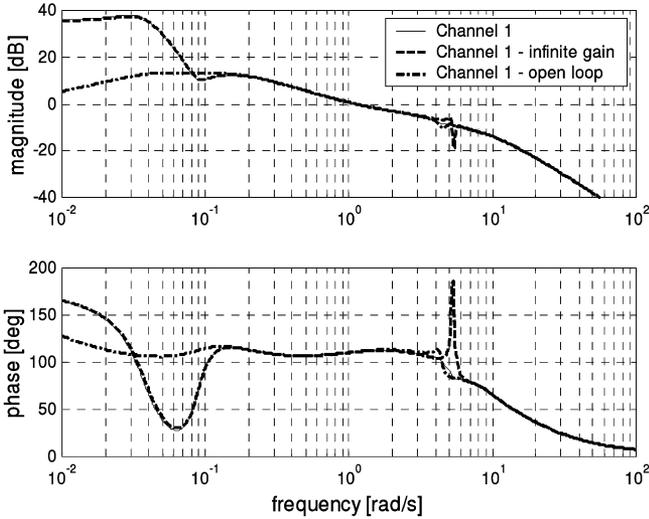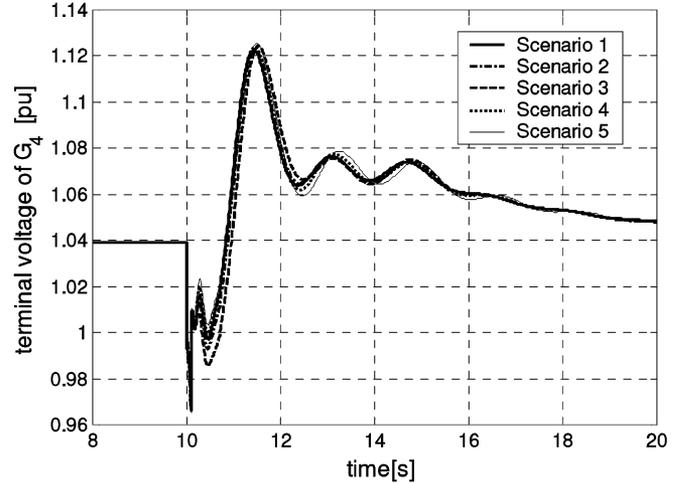
a)
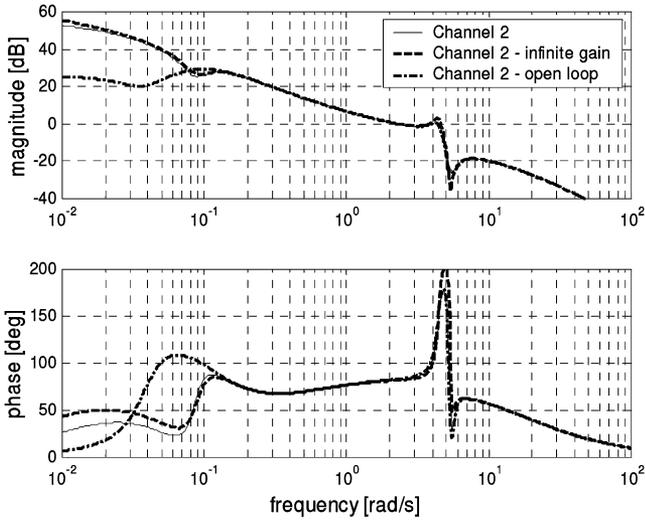
b)

Fig. 11. AVR channels for Design D. (a) Channel 1. (b) Channel 2.

Fig. 12. Response of generator G_4 to 100-ms fault for all five scenarios.

the gain of AVR_3 infinite. The difference between the standard AVR channels and the design AVR channels is small, thereby confirming that the cross-coupling is weak, except at very low frequency. The latter cross-coupling is evident in the difference between the Bode plots of the standard AVR channels and AVR channels with both AVR loops open, channel 1 open loop, and channel 2 open loop, at frequencies less than 0.1 rad/s, as shown in in Fig. 11. The crossover frequencies for the open-loop AVR channels are reduced to roughly 2 rad/s. (Previously, they were roughly 5 rad/s.)

In comparison to design C, the more aggressive oscillation damping by the PSS_3 and PSS_4 designs, (9) and (11), respectively, is observed for design D in Fig. 8 with better PSS channel shapes and stability margins, see Table II. The improvement in oscillation stability in design D is corroborated by the large-signal voltage and speed responses to a 100-ms fault shown in Figs. 6 and 7.

The separation of the individual AVR and PSS designs through the combined step-by-step AVR and PSS design

procedures permits near-optimal design. The AVR and PSS designs are completely coordinated. Design D is close to the limits to overall power system stability performance including oscillation stability performance as well as transient stability performance.

Robustness of PSS/AVR designs to changing power system operating conditions, loading, and changing system topologies is explored in detail in [7]. Here, interest centers on the robustness of the final design D in (8)–(11) to the five different network impedance scenarios in [6, Table I]. Large-signal terminal voltage responses to a symmetrical three phase fault of 100-ms duration near node 5, as shown in Fig. 12, are almost identical. The coordinated PSS/AVR design D is highly robust to all five network scenarios.

VII. CONCLUSION

In this paper, procedures are presented to separate the design of individual PSSs and separate the design of individual AVRs for a strongly coupled multimachine system. Thereby, step-by-step designs of PSS and AVR devices at a given machine can be totally coordinated to achieve near-optimal overall power system stability performance including oscillation stability performance and transient stability performance. This is illustrated by application to two PSSs and two AVRs in the well-known five-machine equivalent of the unstable South/South Eastern Brazilian network. The proposed coordinated PSS/AVR design procedure is established within a frequency-domain framework and serves as a most useful small-signal complement to established large-signal transient simulation studies. It is applicable not only to conventional PSS and AVR devices, but also to similar devices such as the recent PSS2B and PSS4B [5], [22].

APPENDIX A
AVR/PSS SIMULATION MODELS

More detailed models of AVR and PSS, ST3A excitation system and PSS1A, respectively, [22], used in nonlinear simulation for design A, have the following parameters (see Tables III–V). Other designs are similarly implemented.

TABLE III
IEEE ST3A EXCITATION SYSTEM PARAMETERS USED IN DESIGN A

$T_A = 0$	$V_{1MIN} = -0.2$	$K_G = 1.0$
$T_R = 0$	$V_{MMAX} = 1.0$	$K_M = 0.176$
$T_M = 0.058$	$V_{MMIN} = 0$	$K_A = 200.0$
$T_B = 10.0$	$V_{RMAX} = 10.0$	$K_P = 6.15$
$T_C = 1.0$	$V_{RMIN} = -10.0$	$\theta_P = 0°$
$X_L = 0.081$	$V_{GMAX} = 5.8$	$K_I = 0$
$V_{1MAX} = 0.2$	$V_{B\,MAX} = 10.0$	$K_C = 0.2$

TABLE IV
IEEE PSS1A STABILIZER PARAMETERS FOR PSS_3 USED IN DESIGN A

$A_1 = 0.061$	$T_3 = 0.1$	$V_{STMAX} = 0.1$
$A_2 = 0.0017$	$T_4 = 0.012$	$V_{STMIN} = -0.1$
$T_1 = 0.3$	$T_5 = 3.0$	
$T_2 = 0.02$	$K_S = 30.0$	

TABLE V
IEEE PSS1A STABILIZER PARAMETERS FOR PSS_4 USED IN DESIGN A

$A_1 = 0.061$	$T_3 = 0.3$	$V_{STMAX} = 0.1$
$A_2 = 0.0017$	$T_4 = 0.03$	$V_{STMIN} = -0.1$
$T_1 = 0.3$	$T_5 = 3.0$	
$T_2 = 0.03$	$K_S = 60.0$	

APPENDIX B
STEP-BY-STEP DESIGN PROCEDURES
FOR MULTIPLE PSSs AND AVRs

The step-by-step procedure for n-input n-output PSS systems comprising stabilizers $PSS_1, \ldots, PSS_n$ is as follows.

1) Check that the n-input n-output PSS system has no right half-plane transmission zeros.
2) Define the open-loop generator G_i PSS channel, PSS channel i, with PSS_j, $j < i$, previously designed, and with PSS_j, $j > i$, gain chosen to be infinite. (A very high gain would suffice.) This PSS channel has right half-plane zeros only when the n-input n-output PSS system has right half-plane transmission zeros.
3) Design PSS_i so that the gain of the Bode plot for PSS channel i defined in 2) is raised above 0 dB at interarea mode frequency with sizeable stability margins while inducing rapid gain roll off at lower and higher frequencies.
4) Perform steps 2) and 3) for $i = 1$ to n.

The step-by-step procedure for n-input n-output AVR systems comprising regulators $AVR_1, \ldots, AVR_n$ is as follows.

1) Define the open-loop generator G_i AVR channel, AVR channel i, with AVR_j, $j < i$, previously designed, and with AVR_j, $j > i$, gain chosen to be infinite. (A very high gain would suffice.)
2) Design AVR_i so that the gain of the Bode plot for AVR channel i, defined in 2), is high and stabilizes any instability at low frequency. The frequency range over which the open-loop gain is above 0 dB must meet the requirements of the context.
3) Perform steps 1) and 2) for $i = 1$ to n.

REFERENCES

[1] P. Kundur, *Power System Stability and Control*. New York: McGraw Hill, 1994.

[2] F. D. DeMello and C. Concordia, "Concepts of synchronous machine stability as affected by excitation control," *IEEE Trans. Power Appl. Syst.*, vol. PAS-88, no. 2, pp. 316–329, Apr. 1969.

[3] P. Kundur, M. Klein, G. J. Rogers, and M. S. Zywo, "Application of power system stabilizers for enhancement of overall system stability," *IEEE Trans. Power Syst.*, vol. 4, no. 2, pp. 614–626, May 1989.

[4] G. Andersson, P. Donalek, R. Farmer, N. Hatziargyriou, I. Kamwa, P. Kundur, N. Martins, J. Paserba, P. Pourbeik, J. Sanchez-Gasca, R. Schulz, A. Stankovic, C. Taylor, and V. Vittal, "Causes of the 2003 major grid blackouts in North America and Europe, and recommended means to improve system dynamic performance," *IEEE Trans. Power Syst.*, vol. 20, no. 4, pp. 1922–1928, Nov. 2005.

[5] I. Kamwa, R. Grondin, and G. Trudel, "IEEE PSS2B versus PSS4B: The limits of performance of modern power system stabilizers," *IEEE Trans. Power Syst.*, vol. 20, no. 2, pp. 903–915, May 2005.

[6] G. E. Boukarim, S. Wang, J. H. Chow, G. N. Taranto, and N. Martins, "A comparison of classical, robust and decentralized designs for multiple power system stabilizers," *IEEE Trans. Power Syst.*, vol. 15, no. 4, pp. 1287–1292, Nov. 2000.

[7] G. J. W. Dudgeon, W. E. Leithead, A. Dysko, J. O'Reilly, and J. R. McDonald, "The effective role of AVR and PSS in power systems: Frequency response analysis," *IEEE Trans. Power Syst.*, vol. 22, no. 4, pp. 1986–1994, Nov. 2007.

[8] L. Gerin-Lajoie, D. Lefebure, M. Racine, L. Soulieres, and I. Kawa, "Hydro-Quebec experience with PSS tuning," in *1999 IEEE PES Summer Meeting*, Edmonton, AB, Canada, Jul. 1999, pp. 88–95.

[9] N. Martins and L. T. G. Lima, "Eigenvalue and frequency domain analysis of small-signal electromechanical stability problems," *IEEE Special Publication on Eigenanalysis and Frequency Domain Methods for System Dynamic Performance*, pp. 17–33, 1989.

[10] N. Martins, "Efficient eigenvalue and frequency response methods applied to power system small-signal stability studies," *IEEE Trans. Power Syst.*, vol. 1, no. 1, pp. 217–226, Feb. 1986.

[11] D. R. Ostojic, "Stabilization of multimodal electromechanical oscillations by coordinated application of power system stabilizers," *IEEE Trans. Power Syst.*, vol. 6, no. 4, pp. 1439–1445, Nov. 1991.

[12] M. J. Gibbard, N. Martins, J. J. Sanchez-Gasca, N. Uchida, V. Vital, and L. Wang, "Recent applications of linear analysis techniques," *IEEE Trans. Power Syst.*, vol. 16, no. 1, pp. 154–162, Feb. 2001.

[13] M. J. Gibbard and D. J. Vowles, "Reconciliation of methods of compensation for PSSs in multimachine systems," *IEEE Trans. Power Syst.*, vol. 19, no. 1, pp. 463–472, Feb. 2004.

[14] A. Elices, L. Rouco, H. Bourles, and T. Margotin, "Design of robust controllers for damping interarea oscillations: Application to the European power system," *IEEE Trans. Power Syst.*, vol. 19, no. 2, pp. 1058–1067, May 2004.

[15] K. E. Bollinger, R. Winsor, and A. Campbell, "Frequency response methods for tuning stabilizers to damp out tie-line power oscillations: Theory and field- test results," *IEEE Trans. Power Appl. Syst.*, vol. PAS-98, no. 5, pp. 1509–1515, Sep. 1979.

[16] P. Kundur, D. C. Lee, and H. M. Z. El-Din, "Power system stabilizers for thermal units: Analytical techniques and on-site validation," *IEEE Trans. Power Appl. Syst.*, vol. PAS-100, no. 1, pp. 81–95, Jan. 1981.

[17] D. M. Lam and H. Yee, "A study of frequency responses of generator electrical torques for power system stabilizer design," *IEEE Trans. Power Syst.*, vol. 13, no. 3, pp. 1136–1142, Aug. 1998.

[18] Z. Fadlalmoula, S. S. Robertson, J. O'Reilly, and W. E. Leithead, "Individual channel analysis of the turbogenerator with a power system stabilizer," *Int. J. Control*, vol. 69, no. 2, pp. 175–202, 1998.

[19] H. Quinot, H. Bourles, and T. Margotin, "Robust coordinated AVR + PSS for damping large scale power systems," *IEEE Trans. Power Syst.*, vol. 14, no. 4, pp. 1446–1451, Nov. 1999.

[20] G. J. W. Dudgeon, W. E. Leithead, J. O'Reilly, and J. R. McDonald, "Prospects for the decentralised control of small-scale power networks with embedded generation," in *2000 IEEE PES Winter Meeting*, Singapore, Jan. 2000, pp. 1399–1404.

[21] K. T. Law, D. J. Hill, and N. R. Godfrey, "Robust controller structure for coordinated power system voltage regulator and stabilizer design," *IEEE Trans. Control Syst. Technol.*, vol. 2, no. 3, pp. 220–232, Sep. 1994.

[22] *IEEE Recommended Practice for Excitation System Models for Power System Studies*, IEEE Std. 421.5-2005, Apr. 2006.

[23] P. Kundur, J. Paserba, V. Ajjarapu, G. Andersson, A. Bose, C. Canizares, N. Hatziargyriou, D. Hill, A. Stankovic, C. Taylor, T. Van Cutsem, and V. Vittal, "Definition and classification of power system stability," *IEEE Trans. Power Syst.*, vol. 19, no. 2, pp. 1387–1401, May 2004.

[24] W. E. Leithead, S. S. Robertson, and J. O'Reilly, "Design of controllers within the framework of ICAD," in *Proc. Symp. Quantitative Feedback Theory and Other Frequency-Based Methods and Applications*, Glasgow, U.K., Aug. , 1997.

William E. Leithead received the B.Sc. degree in mathematical physics and the Ph.D. degree in theoretical physics from the University of Edinburgh, Edinburgh, U.K., in 1971 and 1976, respectively.

Currently, he is a Professor and the Director of Systems and Control Engineering in the Department of Electronic and Electrical Engineering, University of Strathclyde, Glasgow, U.K. His research interests include power system dynamics and control and integrated design of wind turbines.

Adam Dyśko (M'06) received the M.Sc. degree from the Technical University of Łódź, Łódź, Poland, in 1990 and the Ph.D. degree from the University of Strathclyde, Glasgow, U.K., in 1998.

Currently, he is a Lecturer in the Department of Electronic and Electrical Engineering, University of Strathclyde, Glasgow. His research interests include power system modeling and simulation, power system protection, and power quality.

John O'Reilly (M'81–SM'00) received the B.Sc., Ph.D., and D.Sc. degrees in engineering from Queens University, Belfast, U.K., in 1972, 1976, and 1985, respectively.

Currently, he is a Professor of control engineering in the Department of Electronics and Electrical Engineering, University of Glasgow, Glasgow, U.K. His research interests include power system dynamics and control with renewable energy.